The role of \varkappa -opioid receptor-induced autophagy in stress-driven synaptic alterations

Christos Karoussiotis¹, Aggeliki Sotiriou², Alexia Polissidis³, Alexandra Symeonof¹, Danai Papavranoussi-Daponte¹, Vassiliki Nikoletopoulou⁴, and Zafiroula Georgoussi¹

August 23, 2022

Abstract

Recent evidence has shown that G protein-coupled receptors (GPCRs) are direct sensors of the autophagic machinery and opioid receptors regulate neuronal plasticity and neurotransmission with an as yet unclarified mechanism. Using in vitro and in vivo experimental approaches, this study aims to clarify the potential role of autophagy and x-opioid receptor (x-OR) signaling on synaptic structure and integrity. We hereby demonstrate that the selective x-OR agonist U50,488H, induces autophagy in a time-and dose-dependent manner in neuronal cells by upregulating microtubule-associated protein Light Chain 3-II (LC3-II), Beclin 1 and Autophagy Related Gene 5 (ATG5). Pretreatment of neuronal cells with pertussis toxin blocked the above x-OR-mediated cellular responses. Our molecular analysis also revealed a x-OR-driven upregulation of becn1 gene through ERK1,2-dependent activation of the transcription factor CREB in neuronal cells. Moreover, our studies demonstrated that sub-chronic U50,488H administration in mice causes profound increases of specific autophagic markers in the hippocampus with a concomitant decrease of several pre- and post-synaptic proteins such as spinophilin, postsynaptic density protein 95 (PSD-95) and synaptosomal associated protein 25 (SNAP25). Finally, using acute stress, a stimulus known to increase the levels of the endogenous x-OR ligand dynorphin, we are demonstrating that administration of the x-OR selective antagonist, nor-binaltorphimine (norBNI), blocks the induction of autophagy and the stress-evoked reduction of synaptic proteins in the hippocampus. These findings provide novel insights about the essential role of autophagic machinery into the mechanisms through which x-OR signaling regulates brain plasticity.

Introduction

The \varkappa -opioid receptor (\varkappa -OR), that is distributed in the central and peripheral nervous system mediates the diverse effects of opioids ranging from pain perception, neurotransmitter release and respiratory depression to the regulation of a variety of psychiatric disorders including anxiety and addiction (1). The \varkappa -OR and its endogenous neuropeptide, dynorphin A, were found to play a key role in modulating anxiety and stress-related behaviors. Thus, stress has been shown to increase endogenous dynorphin levels and up-regulate \varkappa -OR signaling in the nucleus accumbens and the CA3 region of the hippocampus (2). Ablation of \varkappa -OR from brain dopaminergic neurons produced anxiolytic effects, confirming that the regulation of dopaminergic neurotransmission by \varkappa -OR is critical for manifestation of stress and anxiety (3).

Recent results also suggest that \varkappa -OR antagonists possess promising antidepressant potential, indicating that the \varkappa -OR and its endogenous neuropeptide ligand, dynorphin A, are critical mediators of stress and mood disorders with specific \varkappa -OR antagonists being currently tested in phase II clinical trials (4-6). However,

¹National Centre for Scientific Research-Demokritos

 $^{^{2}}$ IMBB

³Biomedical Research Foundation of the Academy of Athens

⁴University of Lausanne Faculty of Biology and Medicine

the signaling constituents responsible for the neurobiological responses that regulate these physiological phenomena have yet to deduced.

In the brain, the \varkappa -OR is coupled to pertussis toxin sensitive Gi/o proteins to regulate a variety of downstream effectors including adenylyl cyclase, K⁺ and Ca²⁺channels, phospholipase C, and ERK1/2 phosphorylation (1, 7). Such diverse signaling events are mediated not only by interactions with G proteins but also by other proteins that determine the generated signal and alterations in the trafficking, targeting and fine tuning of this receptor (1, 8, 9).

Macroautophagy, herein referred as autophagy, is a highly conserved degradation process in which proteins and organelles are engulfed in autophagic vesicles and subsequently targeted for degradation in lysosomes (10). Autophagy plays an important role in many organisms upon exposure to stress but is also considered to be an important physiological mechanism in neuronal homeostasis. In neurons, autophagy occurs constitutively under physiological conditions, while impaired autophagy is implicated in many neurodevelopmental and neurodegenerative disorders (11). Recent evidence suggests that autophagy regulates the development and function of axons, dendrites and synapses, whereas aberrations in neuronal autophagy contribute to pathological changes. Autophagy alters the kinetics of neurotransmitter release and the density of synaptic vesicles and is also implicated in the degradation of postsynaptic receptors such as the GABA_A and AMPA receptors (11, 12). Autophagy contributes to such alterations by degrading specific synaptic proteins involved in spine remodeling and retraction suggesting a direct link between autophagy and pruning of synaptic connections. Consequently, the targeting of neuronal autophagy may have great clinical implications in terms of treatment of various psychiatric disorders (13, 14).

Additional findings also suggest that GPCRs are direct regulators of autophagy (15). Previous studies have shown that exposure of SH-SY5Y and endothelial cells to morphine or methamphetamine respectively, induces autophagy through the involvement of opioid receptors by as yet undefined mechanisms (16, 17). Moreover, other studies have shown that morphine dysregulates synaptic balance in the hippocampus via a novel signaling pathway involving reactive oxygen species, endoplasmic reticulum stress and autophagy (18). Although opioid receptors and interacting, Gi/o and Regulators of G protein signaling (RGS) proteins, were shown to play key roles in neuronal signaling (8, 19, 20), it is unknown whether x-OR activation by specific agonists can induce the autophagic machinery in neuronal cells and whether these effects could result in synaptic alterations implicated in stress-related behaviors.

The present study demonstrates a novel signaling pathway via which a specific representative of opioid receptors, \varkappa -OR, induces autophagy resulting in synaptosomal integrity changes. In addition, we show that administration of the \varkappa -OR specific antagonist, norBNI to mice, during acute stress exposure [daily forced swim test (FST)], prevents autophagy induction and stress-induced degradation of synaptic proteins. These results provide a novel insight to the role of this receptor in the regulation of neuronal autophagy and demonstrate that \varkappa -OR-mediated autophagy is responsible for specific changes in stress-induced synaptic alterations.

Materials and Methods

Reagents

Opioid ligands U50,488H, naloxone and nor-BNI (nor-binaltorphimine) were purchased from Tocris Bioscience (Cookson MI, USA). Dynorphin₁₋₁₃, pertussis toxin, bafilomycin A1, phosphatase inhibitors and TRI-reagent for RNA extraction were from Sigma Aldrich (St Louis, MO, USA). Protease inhibitors were from Roche (Roche Diagnostics, Basel, Switzerland). Protein A/G agarose beads and PD98059 (MEKI inhibitor SC-3532) were from Santa Cruz Biotechnology (Santa Cruz, CA, USA). Kapa Hi-Fi PCR, Kapa SYBR Fast QPCR kits for ChIP assay and Real-time PCR respectively were purchased from Kapa Biosystems (Roche, IN, USA). All reagents were purchased from Sigma Aldrich (Sigma Aldrich MI, USA)

Antibodies

Antibodies used for immunoblotting and microscopy analysis were the following: LC3B (CST-2775S), p-

CREB (S133, CST-9198S), CREB (CST-9197S), p-ERK1,2 (CST-9101S), ERK1,2 (CST-9102S), β -actin (CST-8457), β -tubulin (CST-2128) and β -III tubulin (D71G9) and purchased from Cell Signaling Technology Inc (Danvers, MA, USA). Beclin1 (sc-11427), p62 (sc-48402), ATG5 (sc-133158), Neurabin II (sc-14774) and PSD-95 (sc-32290) antibodies were purchased from Santa Cruz Biotechnology (Santa Cruz, CA, USA). All secondary antibodies were from KPL (Maryland, USA). For confocal microscopy the anti-rabbit Alexa-Fluor 568 (Thermo Fisher Scientific, MA, USA) and anti-mouse CFL 488 (Santa Cruz, CA, USA) sera were used.

Cell cultures

Neuro-2A neuroblastoma cells stably expressing the myc-tagged human \varkappa -OR (\varkappa -Neuro-2A) were cultured in Dulbecco's modified Eagle's medium (Merck Millipore, MA. USA) with 2 mM L-glutamine, 100 U/ml penicillin, 100 µg/ml streptomycin and 10% fetal bovine serum (Biosera, France) under humidified atmosphere 5 % CO₂ at 37°C. For the generation of the stable cell line expressing the human myc- \varkappa -OR, Neuro-2A cells were transfected with the h \varkappa -OR in pA3M vector (\varkappa -Neuro-2A). Clonal cell lines stably expressing the \varkappa -OR (260 fmol/mg protein) were established upon selection with G418. The expression levels of \varkappa -OR were determined by [³H]-diprenorphine saturation binding of cell membranes, as described by (50), and western blotting. For the pertussis toxin (PTX) ribosylation experiments, \varkappa -Neuro-2A cells were treated with PTX (100 ng/ml) for 16 h prior of agonist stimulation as described by (19).

Animals and treatments

Animal maintenance and experimentation were conducted in strict compliance with the European and National Law for Laboratory Animal use (Directive 2010/63/EU and Greek Law 161/91), the FELASA recommendations and the ethical and practical guidelines for the care and use of laboratory animals set by the competent veterinary services of Athens. All experiments were carried out in wild-type C57BL/6J mice. Three-month-old male mice were divided into two groups (n=4/ group) and injected intraperitoneally once per day with saline or 5 mg/kg U50,488H for 6 consecutive days. The mice were sacrificed 3 h after the last U50,488H/saline injection and the hippocampus, cortex, and striatum were rapidly dissected on ice. Isolated regions were placed in cold PBS and immediately homogenized by sonication in RIPA buffer containing 50 mM Tris-HCl pH 7.2, 150 mM NaCl, 2 mM EDTA, 1% Triton 100-X, 1 % sodium deoxycholate, 0.5 % SDS and 1 mM dithiothreitol in the presence of protease inhibitors and incubated for 1 h at 4 °C. The resulting supernatant was collected after centrifugation at 8,000 x g for 20 min.

Primary neuronal cultures

Cortices and hippocampi were isolated on embryonic day 16 (E16.5) rinsed and dissected in ice-cold PBS and incubated with 0.25 % trypsin for 25 min at 37 °C. The digestion was terminated by the addition of DMEM solution supplemented with 10 % FBS followed by trituration tissue dissociation. The resulting cells were centrifuged for 5 min at 800 rpm and neurons dissolved in Neurobasal medium supplemented with 2 % B-27, 0.5 mM L-glutamine and 1 % penicillin/streptomycin. The cells were plated at a density of $2x10^5$ cells/well in 6-well poly-L-lysine-coated tissue culture dishes or on coverslips where necessary. Cells were cultured for 10 days (DIV10) for neuron maturation under 5 % CO_2 at 37°C. Neuronal purity was >90 % as determined by immunofluorescence using the neuronal marker β III-tubulin.

Isolation of synaptosomes

Synaptosomes were isolated as previously described by (51). Briefly, mice at postnatal days 90-95 were treated as described above. Brain hippocampi from the two animal groups were collected, rinsed and homogenized in solution A, consisting of 0.32 M Sucrose, 1 mM NaHCO₃, 1 mM MgCl₂, 0.5 mM CaCl₂*H2O, 10 mM sodium pyrophosphate and protease inhibitors using a dounce homogenizer. After centrifugation at 1,400 x g for 10 min at 4 °C, the resulting supernatants were kept and the pellets were diluted 10 % w/v in solution A and spun at 710xg for 10 min. The supernatants were collected and centrifuged at 13,800 x g for 10 min at 4 °C. The pellets were resuspended in 0.32 M sucrose and 1 mM NaHCO₃ using a dounce homogenizer and layered on a discontinuous sucrose gradient (10ml-layers of 1.2 M, 1.0 M and 0.85 M sucrose). After centrifugation at 82,500 x g for 2 h, the synaptosomes from U50,488- or saline-injected mice were isolated

from the 1.2-1 M sucrose layer.

Western blotting

Neuronal cells treated or not with different \varkappa -OR ligands were rinsed in PBS containing 0.1 mM PMSF and 0.1 mM Na₃VO₄. Cells were lysed in buffer containing 25 mM Tris pH 7.4, 150 mM NaCl, 5 mM EDTA, 1 % Igepal, 1 mM dithiothreitol and 1 % of a protease and phosphatase inhibitor cocktail. Proteins were separated on 10 or 17 %-SDS-PAGE and transferred onto PVDF membranes (Immobilon-P, Merck Millipore, MA, USA) as described by (8). Blots were visualized using enhanced chemiluminescence (Pierce-Thermo Scientific, MA, USA) and a luminescent image analyzer (Fujifilm LAS-4000). The densitometric analyses were performed using ImageJ software (National Institute of Health, Bethesda, MD, USA). β -Actin and β -tubulin were used as loading controls for protein analysis.

Detection of MAP and JNK phosphorylations

 κ -Neuro-2A cells were cultured in 60 mm plates for 48 h in the presence or absence of U50,488H (20 μM) for 15min and 6 h at 37°C. Cell monolayers were rinsed with PBS following the procedure as described by (43). Where necessary cells were exposed to the ERK1, 2 inhibitor PD98059 (20 μM for 45 min), or the JNK inhibitor SP600125 (20 μM for 30 min) prior to agonist treatment. The proteins were resolved in 10 % SDS-PAGE and visualized by immunoblotting with the appropriate antibodies as described previously by (50).

Immunofluoresence staining

Primary neuronal cultures on poly-L-lysine coated coverslips were treated with α-OR ligands for different time intervals. Cells were fixed for 10 min with 100 % methanol at ⁻20°C and incubated overnight at 4 °C with the anti-LC3B antibody (1:200) followed by 2 h incubation with the fluorescein-conjugated secondary antibody Alexa fluor 488 goat anti-rabbit (1:100) and TO-PRO-3 (1:500) for nuclear staining. The cells were mounted on slides with Vectashield mounting media (Vector Laboratories Inc., Burlingame, CA, USA) and visualized using a Leica SP8 confocal microscope (Leica Microsystems, Germany).

Co-immunoprecipitation assay

Hippocampi from wild-type C57BL/6J mice were isolated and lysed in RIPA lysis buffer containing 1% v/v Triton X-100, 0.2% w/v SDS, 1% w/v sodium deoxycholate, 50 mM Tris-HCl (pH 7.6), 5 mM EDTA, 150 mM NaCl, 50 mM NaF, supplemented with antipain, leupeptin, benzamidine (1 µg/ml each), complete EDTA-free inhibitors, 1 mM PMSF and 1 mM sodium orthovanadate. Approximately 800 µg of the clarified cell lysates were incubated with an LC3B monoclonal antibody (2 µg) overnight at 4 °C. Normal rabbit serum (NRS) was used as control. Immune complexes were recovered on protein A agarose beads for 3 hours at 4 °C, washed extensively with buffer consisted of 25 mM Tris-HCl (pH 7.4), 300 mM NaCl, 1 mM EGTA, 1 mM EDTA, 1 % Triton X-100, 0.2 mM PMSF and 0.2 mM Na₃VO₄, subjected to SDS-PAGE and transferred onto polyvinylidene (PVDF) membranes. Immunoprecipitation of cell lysate proteins was verified by immunoblotting using the appropriate antibodies.

Chromatin immunoprecipitation

x-Neuro-2A cells treated or not with U50,488 for 6 h were cross-linked with 1 % formaldehyde for 10 min at room temperature followed by 5 min incubation with 0.125 mM glycine as previously described (52). Briefly, isolated nuclei were sonicated and the extracted chromatin (200 μg) supplemented with protease inhibitors was immunoprecipitated using a ChIP grade antibody against CREB or NRS. The crosslinked protein complexes were incubated for 2 h at 4 °C under rotation with pre-blocked salmon sperm DNA and 5 % BSA protein A/G agarose beads. Following extensive washes with 0.1 % SDS, 1 % Triton X-100, 2 mM EDTA, 150 mM NaCl, 20 mM Tris-HCl, the immune complexes were incubated overnight in 1 % SDS, 100 mM NaHCO3 and proteinase K. The immunoprecipitated DNA was extracted by phenol-chloroform-isoamylyl alcohol and PCR was carried out using the following primers for Beclin1, BECN1 (forward) 5'-CGGGTAAACAGGGATCT-GGAG-3' and (reverse) 5'-GCCAGGGACTCTAGGCTTCTT-3', spanning

the putative CRE binding site in the mouse Becn1 promoter. The PCR products were separated on 2 % agarose gels.

RNA extraction and real-time polymerase chain reaction

Total RNA was extracted with TRI-reagent from control or U50,488H treated \varkappa -Neuro-2A cells according to manufacturer's instructions. Total RNA (1 μ g) was used as template for cDNA synthesis using SuperScript II reverse transcriptase (Thermo Fisher). The following primers were designed for Real Time-PCR: Becn1,(forward):5'-GGCCAATAAGATGGGTCTGA-3'; (reverse) 5'-GCTGCACACAGTCCAGAAAA-3'; for ATG5, 5' (forward) AAGTCTGTCC-TTCCGCAGTC-3'; (reverse) GAAGAAAGTTATCTGGGTAGCTCA-3'; for GAPDH (forward) 5'-TGTGTCCGTCGTGGATCTGA-3', (reverse) 5'-CCTGCTTCACCACCTTCT-TGA-3', using a MX3000P QPCR System (Stratagene, La Jolla, CA, USA). The expression of the mRNAs was calculated using the Δ Ct method.

Forced swim test

The forced swim test (FST) was adapted from McLaughlin et al. (24) with minor modifications. Briefly mice were divided into 4 groups (n=6/group) and on day 1, they were injected intraperitoneally with the κ -OR antagonist, nor-BNI (10 mg/kg), or vehicle and placed in a 5 L beaker (40 cm tall \times 25 cm in diameter) filled with 2.5 L of 30 °C water for a single swim trial of 15 min. On day 2, the animals were subjected to 4x FST trials, 6 min long, with 6 min intervals. During the last 4 min of the trial mice were recorded and the time spent immobile was counted as "stressed behavior". After each trial, the mouse was removed from the water, dried with towels and returned to its home cage for at least 6 min before further testing. Immobility was defined as the animal remaining motionless or making only minor non-escape-related movements. To qualify as immobility each posture must be clearly visible and sustained for a minimum of 2 seconds. Immobility was measured with the specialized video tracking software Ethovision XT9.0 (Noldus, Netherlands). Difficulty in swimming or staying afloat were criteria for exclusion, however, no mice met these criteria in this study.

Statistical analysis

Statistical analysis was performed using one or two-way analysis of variance (ANOVA) following by Tukey's t test for post-hoc comparisons. All experiments were repeated at least three times. Bands were quantified by densitometric analysis using Image J software (National Institute of Health, Bethesda, MD, USA) and expressed as mean \pm SEM. Representative experiments are shown and statistical significance is shown in each figure legend.

Results

Σελεςτιε κ-ΟΡ αγονιστς ινδυςε τηε αυτοπηαγις φλυξ ιν νευροναλ ςελλς. It is known that neuronal autophagy is involved in cell growth, survival and synaptic plasticity (11, 13). Here, we investigated whether specific κ-OR agonists could trigger autophagy in neuronal cells and modulate synaptic organization. We thus treated Neuro-2A cells, stably expressing κ-OR, with U50,488H, a κ-OR-specific agonist, and monitored the levels of the lipidated LC3 (LC3-II), a reliable and specific marker of autophagosome formation located at the membrane of the autophagosome. As shown in Fig. 1A, increasing concentrations of U50,488H for 6 h caused a dose-dependent increase in LC3-II accumulation. Addition of the lysosomal inhibitor bafilomycin A1 (BafA1), which prevents the fusion of autophagosomes with lysosomes indicated a significant increase in LC3-II levels in cells exposed simultaneously to U50,488H and BafA1, relative to BafA1 alone (Fig. 1B), indicating that κ-OR activation upregulates the autophagic flux. Finally, LC3-II accumulation was markedly reversed upon treatment with the opioid antagonist, naloxone, prior to U50,488H exposure, further confirming the κ-OR-dependent autophagic activation (Fig. 1C).

To recapitulate U50,488H-mediated autophagy in a native neuronal milieu, we treated cortical neuronal cultures to U50,488H, that resulted in a significant increase of LC3-positive autophagosomes that appeared as puncta, compared with untreated controls (Fig. 1D, images a, e); an effect that was abrogated when cells were pre-treated with naloxone (images e, i). Consistent with these findings, immunoblot analysis of primary neuronal cultures showed that naloxone blocked the increase in LC3-II accumulation caused by U50,

488H exposure (Fig. 1E). Collectively, these results demonstrate that \varkappa -OR activation induces autophagy in neuronal cells.

To deduce whether \varkappa -OR agonists exert similar effects on autophagy initiation, we exposed Neuro-2A cells to varying concentrations of the endogenous \varkappa -OR neuropeptide dynorphin₁₋₁₃, which also resulted in increased LC3-II and Beclin 1 levels (Fig. 2A, B). This effect was blocked by the selective \varkappa -OR antagonist nor-BNI (Fig. 2C). Finally, dynorphin₁₋₁₃-treated primary neuronal cultures indicated an increase of LC3-positive puncta compared to control neurons (Fig. 2D compare images a with e). These data suggest that \varkappa -OR-induced autophagy is not selective to U50,488H, but can also be mediated by the endogenous \varkappa -OR neuropeptide dynorphin.

Because a key initial event of the autophagosome biogenesis is the formation of the pre-autophagosomal structure (PAS), composed of ULK1, which is a complex of a serine/threonine protein, with the focal adhesion kinase (FIP200) and other proteins, we examined the timing of U50,488H-mediated early autophagic events. Treatment of primary neuronal cultures with U50,488H for 1, 6, and 24 h, triggered a marked increase of FIP200 and ULK1 protein levels reaching a peak at 6 h agonist exposure (Fig. 3A). In parallel, U50,488H treatment of Neuro-2A cells for various time intervals indicated a time-dependent increase of Beclin1, a key mediator of autophagosome formation. This increase peaked at 6 h following U50,488H administration (Fig. 3B). Similarly, as shown in Fig. 3C, exposure of Neuro-2A cells to U50,488H increased the protein levels of ATG5 and Beclin 1, with a concomitant decrease of p62 known to increase when autophagy is inhibited and decrease when autophagy is induced (21). Additionally, Becn1 and Atg 5 mRNA levels were also elevated after 6 h U50,488H cell exposure (Fig. 3D). These results clearly demonstrate that \varkappa -OR is involved in autophagosome biogenesis in neuronal cells.

Ιδεντιφιζατιον οφ τηε x-OP σιγναλινη πατηωαψ τηατ ρεγυλατες τηε αυτοπηαγις μαςηνερψ. The x-OR is coupled to pertussis toxin-sensitive Gi/o proteins to regulate a variety of effectors (1, 8). To define the role of G proteins, we pretreated Neuro-2A cells with pertussis toxin (PTX), which ribosylates Gαi/o subunits. PTX blocked U50,488H-mediated increase of LC3-II and Beclin 1 levels (Fig. 4A, B), suggesting that Gi/o proteins are important players in x-OR-mediated autophagy. To examine whether ERK1,2 is implicated in x-OR- induction of autophagy the levels of ERK1,2 phosphorylation of Neuro-2A cells were assessed in the presence or absence of PTX. U50,488H enhanced ERK1,2 phosphorylation after 15 min and 6 h post-exposure and this effect was abolished by PTX exposure (Fig. 4C). Moreover, when the cells were pretreated with the ERK1,2 inhibitor PD98059 prior to agonist activation, U50,488H-mediated-ERK1,2 phosphorylation was abolished with a concomitant decrease of the LC3-II and Beclin1 levels, relative to the untreated cells (Fig. 4D). On the other hand, JNK activation cannot recapitulate the effects of ERK1,2 phosphorylation on x-OR-mediated induction of the autophagic pathway. Indeed, no effects on LC3-II accumulation were detected in U50,488H-treated cells relative to the untreated ones upon pre-treatment with the JNK inhibitor SP600125 (Fig. 4E). These results suggest that ERK1,2 is implicated in x-OR-mediated autophagy.

x-OP ρεγυλατες Βεςλιν1 τρανσςριπτιον ια "PEB αςτιατιον. Because it is known that CREB regulates various autophagic genes (22) and that a consensus CRE binding site (TGACGTCA) exists in the mouse *Becn1* promoter, we sought to determine if autophagic genes are regulated by p-CREB upon U50,488H exposure. CREB was phosphorylated in response to U50,488H cell exposure, and this effect was abolished by the ERK1,2 inhibitor PD98059 (Fig. 4F). Moreover, chromatin immunoprecipitation (ChIP) assay in isolated chromatin fragments of Neuro-2A cells indicated that CREB binding in the *Becn1* promoter was greatly enhanced by U50,488H exposure relative to untreated cells (Fig. 4G). Therefore, α-OR-mediated increase in Beclin1 levels appears to involve transcriptional activation of the beclin1 gene by ERK1,2-activated CREB.

U50,488H administration induces autophagy and promotes synaptic alterations in mouse hippocampus. We next sought to examine whether we could recapitulate U50,488H-mediated α-OR autophagy in vivo and determine whether specific brain regions are involved. To this end, mice were injected with saline (vehicle) or U50,488H for 7 consecutive days and the levels of LC3-II and Beclin1 were measured in the hippocampus, cortex and striatum. U50,488H resulted in a significant increase of LC3-II and Beclin1 in the mouse hippocampus as compared to vehicle, but with no significant changes in cortical and striatal lysates (Fig. 5A-C). Collectively, these results suggest that x-OR-mediated autophagy is detected specifically to the mouse hippocampus.

Autophagy contributes to synaptic plasticity by degrading specific proteins that are essential for synaptic function and spine remodeling (13). To elucidate whether U50,488H-mediated autophagy leads to synaptic alterations, initially the levels of proteins enriched in dendritic spines such as PSD-95 and spinophilin, were examined in the hippocampus, cortex and striatum of U50,488H-treated mice. As shown in Fig. 5D, spinophilin and PSD-95 in hippocampal lysates were significantly decreased in U50,488H-treated mice compared with saline-treated controls. However, no significant alterations for these proteins were detected in the cortex or striatum (Fig. 5E, F). This was further confirmed in isolated synaptosomes where a pronounced decrease of spinophilin, PSD-95, as well as SNAP25 was detected in U50,488H-injected mice, as compared to control ones (Fig. 5G). All these suggest that these synaptic proteins are degraded, possibly by being engulfed in the \varkappa -OR-mediated autophagic cargo.

To test this hypothesis and in view of the known interaction of LC3 with autophagic cargos through the LC3-interacting regions (LIR) of various proteins, spinophilin, SNAP25 and PSD-95 among them (13, 23), we examined whether these proteins interact with LC3. Co-immunoprecipitation studies of hippocampal lysates using an LC3 antibody indicated that spinophilin, PSD-95 and SNAP25 do interact with LC3 (Fig. 6A). Moreover, to further define whether these synaptic protein alterations are indeed due to autophagy induction we measured their levels in the presence of BafA1. Treatment of Neuro-2A cells with U50,488H decreases the levels of spinophilin and PSD95. Inhibition of autophagy by BAF1 treatment did not alter these protein levels, suggesting that U50,488H-x-OR activation indeed leads to degradation of these synaptosomal proteins (Fig. 6B). Finally, to verify whether these x-OR-mediated effects are due to alterations in neuronal sprouting, the number of branches in U50,488H-treated hippocampal neuronal cultures were measured. U50,488H significantly reduced the number of branches relative to the controls (Fig. 6C), suggesting that x-OR-induced autophagy modulates neuronal morphogenesis, possibly by degrading key synaptic proteins.

Aςτιατιον οφ της ενδογενους χ- $OP/\delta \psi$ νορπηιν σψστεμ υπον στρεσς υπρεγυλατες αυτοπηαγύ ιν της ηιπποςαμπυς ανδ ρεσυλτς ιν σύναπτις αλτερατιονς. It is well documented that the x-OR/dynorphin system plays an important role in anxiety and stress-related behaviors and that x-OR antagonists exhibit anxiolytic effects (24, 25). To examine whether stress-induced endogenous dynorphin release impacts on autophagy regulation, we examined the consequences of acute stress on autophagy in the hippocampus. To this end, mice injected with either vehicle or the x-OR selective antagonist, nor-BNI, which is known to exert anxiolytic effects, were subjected to a two-day modified forced swim test (FST) (Fig. 7A). Male C57BL/6J mice were divided into 4 groups saline-control or saline-FST (stressed) and norBNI-not stressed or nor-BNI-FST (stressed). nor-BNI significantly decreased immobility time following the FST, compared to saline-treated mice, suggesting that nor-BNI attenuates stress-related behavior (Fig. 7B). Subsequently, the levels of the autophagic markers LC3-II and Beclin1 were measured in isolated hippocampal lysates and found to be significantly increased in stressed animals (FST) relative to vehicle injected-non-stressed ones (Fig. 7C). In contrast, this increase in autophagic markers was not detected in nor-BNI-treated mice under control or FST conditions when compared with the saline-control group (Fig. 7C). Moreover, as expected, no significant alterations of LC3-II levels were detected in the cortices of the same treatment groups (Fig. 7D), confirming that the hippocampus is the target region for x-OR-induced autophagy under acute stress.

Finally, to confirm that dynorphin/x-OR-induced autophagy-mediated changes in the structural reorganization of hippocampal synapses during stress may be rescued by nor-BNI, we measured the levels of synaptic proteins in hippocampi of stressed and naïve animals subjected to nor-BNI, or saline treatment. Our results demonstrated that spinophilin, PSD-95, and SNAP-25 protein levels were significantly reduced in stressed animals relative to the control ones (Fig. 7E). In contrast, the levels of these synaptic proteins in nor-BNI injected mice prior to FST were at the same levels as the control nor-BNI-injected ones devote of the stressor

(Fig. 7E, lanes 5-8). Again, no significant alterations in cortical lysates of these proteins were detected, irrespective of the stress-related regime or nor-BNI administration status (Fig. 7F). Collectively, these results suggest that the endogenous dynorphin release due to the acute FST results in \varkappa -OR-mediated induction of autophagy that in turn leads to aberrant hippocampal synaptic alterations.

Discussion

Previous studies have shown that in the brain the x-OR is involved in motivation, stress-related responses and adult neurogenesis and that x-OR agonists and antagonists exert potent pro- and anti-depressant effects, respectively, in rodents (6, 26). However, the mechanistic details of the aberrant synaptic function and resulting behavior mediated by x-OR upon stress remain elusive. In the present study, we demonstrate that x-OR plays a role in stress-induced autophagy, which leads to synaptic alterations. x-OR-induced autophagy occurs primarily in the hippocampus despite x-OR's high expression levels in cortex and striatum. Gi/o proteins and U50,488H-induced ERK1,2 activation are responsible for κ-OR-mediated autophagy. An intriguing finding of the present study has been that U50,488H-dependent-CREB activation regulates the transcription of the becn1 gene, confirming that \varkappa -OR activation leads to transcriptional induction of specific autophagic genes. We are thus proposing a putative G protein dependent signaling pathway for the control of autophagy by x-OR. Activated x-OR leads to activation of ERK1,2 which phosphorylates CREB, with the later promoting alterations of autophagic genes leading to synaptic protein changes (Fig. 8). This proposal is in agreement with previous observations which have shown that heterotrimeric G proteins control autophagic sequestration in HT-29 cells (27, 28), and that $G\alpha i3$, which is activated by \varkappa -OR (8), plays a crucial role in autophagosomal membrane compartmentalization (29) and autophagy initiation (30). It is also compatible with previous findings suggesting that a dynamic interplay between Gai3, the activator of G-protein signaling 3 and Gα-interacting vesicle-associated protein (GIV), are signaling components that determine whether autophagy is induced or inhibited (31), and that Gai3 interacts with RGS4 to inhibit autophagy (32).

A number of different GPCRs have been shown to regulate autophagy albeit through different mechanisms (15). Thus, dopamine D2 and D3 receptors were shown to be positive regulators of autophagy, involving the Akt-mTOR and AMP-activated protein kinase (AMPK) signaling pathways (33). Similarly, activation of the β 2-adrenergic receptor upregulates autophagy and increases collagen degradation in order to maintain cardiac extracellular matrix homeostasis (34). Methamphetamine exposure also induces autophagy via the α -OR as a pro-survival response against apoptotic endothelial cell death, an effect that is also mediated by ERK1,2 activation and inactivation of the Akt/mTOR pathway (16). In the mouse hippocampus, acute or chronic morphine administration upregulates autophagic flux as protective response towards morphine-induced neuronal death and consequent spatial memory deficits (35). Moreover, chronic morphine administration alters synaptic plasticity in the hippocampus and results in spine and excitatory synapse density reduction, via generation of reactive oxygen species leading to Endoplasmic Reticulum (ER) stress activation (18). Finally, it was noted that morphine-mediated autophagy involves activation of ER stress with subsequent downstream astrocyte activation via the μ -opioid receptor (36), a finding confirming that opioids are indeed potential positive regulators of autophagy.

The immediate responses to stressful stimuli include neuro-morphological changes in multiple brain areas including the hippocampus (37). Acute stress reduces the density of dendritic spines, alters the location of postsynaptic elements of excitatory synapses, and impairs long-term potentiation and memory (14, 37). Chronic stress has been reported to enhance autophagy in rodents (38, 39). Furthermore, a role for autophagy in depressive-like behaviors and cognitive impairment has been demonstrated following prenatal stress (40). Our current findings extend the existing evidence by demonstrating a plausible scenario whereas the dynorphin/x-OR system initiates autophagy, which leads to stress-induced synaptic alterations.

Neuronal autophagy plays a major role in brain function by modulating synaptic organization and morphogenesis (12, 13). It contributes to synaptic plasticity by degrading specific synaptic proteins such as PSD-95, PICK1 and SHANK3, which play important roles in synaptic function and spine modeling. This implies a direct link between autophagy and pruning of synaptic connections during postnatal development (13).

In agreement with these predictions, our findings demonstrate that U50,488H-x-OR activation of primary neuronal hippocampal cultures reduces the number of neurite branches. In addition, sub-chronic U50,488H administration in mice led to degradation of the key scaffolding synaptic proteins, spinophilin, PSD95 and SNAP25, particularly in the hippocampus, but not in the cortex or striatum. We specifically chose to examine these proteins as they are implicated in dendritic spine remodeling. Spinophilin localizes in the postsynaptic compartment, is enriched in dendritic spines, and modulates spine morphogenesis and maturation through the regulation of the actin cytoskeleton (41). It also interacts directly with opioid receptors and other GPCRs to regulate their trafficking and signaling that leads to synaptic alterations (41-43). On the other hand, SNAP-25 plays a crucial role pre-synaptically by mediating synaptic vesicle fusion. Of note is that SNAP-25 and PSD-95 are substrates of autophagic degradation modulating dendritic spine morphology and function (44).

Stress blocks long term potentiation through release of endogenous opioids including the release of the endogenous x-opioid neuropeptide, dynorphin. Activation of x-OR in vivo promotes aversion, dysphoria, depression, and anxiety-like behaviors (5, 6, 45, 46). Conversely, x-OR antagonists prevent many effects of stress and counteract stress-induced behavioral responses and for this reason, are considered as novel therapeutics for stress-related disorders (4, 47). Forced swim stress in rats elevates dynorphin A levels in the hippocampus [2], while chronic autophagy deficiency in dopamine neurons results in increased size of axon profiles, increased evoked dopamine release and rapid presynaptic recovery [12]. Another interesting finding of the present study has been that FST in mice promoted autophagy, as indicated by the elevated levels of autophagic markers and this effect was prevented by administration of the x-OR antagonist, nor-BNI. This suggests that the endogenous dynorphin/x-OR system is involved in stress-induced autophagy and could be part of the orchestration of structural changes observed in the hippocampus under stress exposure. Interestingly, a concomitant decrease of the three synaptic proteins, spinophilin, PSD-95 and SNAP-25, was also detected in the hippocampus but not the cortex of stressed animals. We thus postulate that degradation of these synaptic proteins could be attributed to their engulfment in the autophagosome. These findings are further supported by the observation that LC3 interacts with these three key protein substrates that possess putative LIR motifs in their sequence. In turn, this suggests that under acute stress, the release of dynorphin triggers the autophagic machinery leading to synaptosomal alterations in the hippocampus. It is interesting to note that similar synaptosomal alterations that are crucial for dendritic spine remodeling and are caused by autophagic degradation have also been reported previously under conditions of nutritional stress, through a BDNF-regulated mechanism (13). Autophagy was also reported to play a crucial role in postnatal spine pruning in layer V pyramidal neurons (48), suggesting that it plays a significant role in synaptic organization and morphogenesis.

Based on the present findings, we conclude that an interplay exists between \varkappa -OR-mediated autophagy and stress-mediated synaptosomal alterations. Indeed, we propose the existence a signaling pathway (Fig. 8) correlating \varkappa -OR-induced autophagy in neurons with synaptic hippocampal alterations under stress conditions. This \varkappa -OR-mediated autophagy mechanism results in synaptic dysfunction in hippocampus that may contribute to the cognitive changes observed upon stress exposure. Given that \varkappa -OR antagonists (47, 49) are in phase II clinical trials for stress-related mood and anxiety disorders, it would be interesting to explore whether these drugs effectively alleviate stress-related pathologies via \varkappa -OR-mediated-autophagy.

References

- 1. Bruchas MR, Land BB, Chavkin C. The dynorphin/kappa opioid system as a modulator of stress-induced and pro-addictive behaviors. Brain Res. 2010;1314:44-55.
- 2. Shirayama Y, Ishida H, Iwata M, Hazama GI, Kawahara R, Duman RS. Stress increases dynorphin immunoreactivity in limbic brain regions and dynorphin antagonism produces antidepressant-like effects. J Neurochem. 2004;90(5):1258-68.
- 3. Van't Veer A, Carlezon WA, Jr. Role of kappa-opioid receptors in stress and anxiety-related behavior. Psychopharmacology (Berl). 2013;229(3):435-52.

- 4. Rorick-Kehn LM, Witkin JM, Statnick MA, Eberle EL, McKinzie JH, Kahl SD, et al. LY2456302 is a novel, potent, orally-bioavailable small molecule kappa-selective antagonist with activity in animal models predictive of efficacy in mood and addictive disorders. Neuropharmacology. 2014;77:131-44.
- 5. Hang A, Wang YJ, He L, Liu JG. The role of the dynorphin/kappa opioid receptor system in anxiety. Acta Pharmacol Sin. 2015;36(7):783-90.
- Lutz PE, Kieffer BL. Opioid receptors: distinct roles in mood disorders. Trends Neurosci. 2013;36(3):195-206.
- 7. Schulz R, Eisinger DA, Wehmeyer A. Opioid control of MAP kinase cascade. Eur J Pharmacol. 2004;500(1-3):487-97.
- 8. Papakonstantinou MP, Karoussiotis C, Georgoussi Z. RGS2 and RGS4 proteins: New modulators of the kappa-opioid receptor signaling. Cell Signal. 2015;27(1):104-14.
- 9. Georgoussi Z, Georganta EM, Milligan G. The other side of opioid receptor signalling: regulation by protein-protein interaction. Curr Drug Targets. 2012;13(1):80-102.
- 10. Chen Y, Klionsky DJ. The regulation of autophagy unanswered questions. J Cell Sci. 2011;124(Pt 2):161-70.
- 11. Nikoletopoulou V, Papandreou ME, Tavernarakis N. Autophagy in the physiology and pathology of the central nervous system. Cell Death Differ. 2015;22(3):398-407.
- 12. Hernandez D, Torres CA, Setlik W, Cebrian C, Mosharov EV, Tang G, et al. Regulation of presynaptic neurotransmission by macroautophagy. Neuron. 2012;74(2):277-84.
- 13. Nikoletopoulou V, Sidiropoulou K, Kallergi E, Dalezios Y, Tavernarakis N. Modulation of Autophagy by BDNF Underlies Synaptic Plasticity. Cell Metab. 2017;26(1):230-42 e5.
- 14. Shen DN, Zhang LH, Wei EQ, Yang Y. Autophagy in synaptic development, function, and pathology. Neurosci Bull. 2015;31(4):416-26.
- 15. Wauson EM, Dbouk HA, Ghosh AB, Cobb MH. G protein-coupled receptors and the regulation of autophagy. Trends Endocrinol Metab. 2014;25(5):274-82.
- 16. Ma J, Wan J, Meng J, Banerjee S, Ramakrishnan S, Roy S. Methamphetamine induces autophagy as a pro-survival response against apoptotic endothelial cell death through the Kappa opioid receptor. Cell Death Dis. 2014;5:e1099.
- 17. Zhao L, Zhu Y, Wang D, Chen M, Gao P, Xiao W, et al. Morphine induces Beclin 1- and ATG5-dependent autophagy in human neuroblastoma SH-SY5Y cells and in the rat hippocampus. Autophagy. 2010;6(3):386-94.
- 18. Cai Y, Yang L, Hu G, Chen X, Niu F, Yuan L, et al. Regulation of morphine-induced synaptic alterations: Role of oxidative stress, ER stress, and autophagy. J Cell Biol. 2016;215(2):245-58.
- 19. Georganta EM, Tsoutsi L, Gaitanou M, Georgoussi Z. delta-opioid receptor activation leads to neurite outgrowth and neuronal differentiation via a STAT5B-Galphai/o pathway. J Neurochem. 2013;127(3):329-41.
- 20. Pallaki P, Georganta EM, Serafimidis I, Papakonstantinou MP, Papanikolaou V, Koutloglou S, et al. A novel regulatory role of RGS4 in STAT5B activation, neurite outgrowth and neuronal differentiation. Neuropharmacology. 2017;117:408-21.
- 21. Bjorkoy G, Lamark T, Pankiv S, Overvatn A, Brech A, Johansen T. Monitoring autophagic degradation of p62/SQSTM1. Methods Enzymol. 2009;452:181-97.

- 22. Seok S, Fu T, Choi SE, Li Y, Zhu R, Kumar S, et al. Transcriptional regulation of autophagy by an FXR-CREB axis. Nature. 2014;516(7529):108-11.
- 23. Johansen T, Lamark T. Selective Autophagy: ATG8 Family Proteins, LIR Motifs and Cargo Receptors. J Mol Biol. 2020;432(1):80-103.
- 24. McLaughlin JP, Marton-Popovici M, Chavkin C. Kappa opioid receptor antagonism and prodynorphin gene disruption block stress-induced behavioral responses. J Neurosci. 2003;23(13):5674-83.
- 25. Fava M, Memisoglu A, Thase ME, Bodkin JA, Trivedi MH, de Somer M, et al. Opioid Modulation With Buprenorphine/Samidorphan as Adjunctive Treatment for Inadequate Response to Antidepressants: A Randomized Double-Blind Placebo-Controlled Trial. Am J Psychiatry. 2016;173(5):499-508.
- 26. Kibaly C, Xu C, Cahill CM, Evans CJ, Law PY. Non-nociceptive roles of opioids in the CNS: opioids' effects on neurogenesis, learning, memory and affect. Nat Rev Neurosci. 2019;20(1):5-18.
- 27. Ogier-Denis E, Couvineau A, Maoret JJ, Houri JJ, Bauvy C, De Stefanis D, et al. A heterotrimeric Gi3-protein controls autophagic sequestration in the human colon cancer cell line HT-29. J Biol Chem. 1995;270(1):13-6.
- 28. Ogier-Denis E, Houri JJ, Bauvy C, Codogno P. Guanine nucleotide exchange on heterotrimeric Gi3 protein controls autophagic sequestration in HT-29 cells. J Biol Chem. 1996;271(45):28593-600.
- 29. Gohla A, Klement K, Nurnberg B. The heterotrimeric G protein G(i3) regulates hepatic autophagy downstream of the insulin receptor. Autophagy. 2007;3(4):393-5.
- 30. Gotthardt D, Blancheteau V, Bosserhoff A, Ruppert T, Delorenzi M, Soldati T. Proteomics fingerprinting of phagosome maturation and evidence for the role of a Galpha during uptake. Mol Cell Proteomics. 2006;5(12):2228-43.
- 31. Garcia-Marcos M, Ear J, Farquhar MG, Ghosh P. A GDI (AGS3) and a GEF (GIV) regulate autophagy by balancing G protein activity and growth factor signals. Mol Biol Cell. 2011;22(5):673-86.
- 32. Bastin G, Dissanayake K, Langburt D, Tam ALC, Lee SH, Lachhar K, et al. RGS4 controls Galphai3-mediated regulation of Bcl-2 phosphorylation on TGN38-containing intracellular membranes. J Cell Sci. 2020;133(12).
- 33. Wang D, Ji X, Liu J, Li Z, Zhang X. Dopamine Receptor Subtypes Differentially Regulate Autophagy. Int J Mol Sci. 2018;19(5).
- 34. Aranguiz-Urroz P, Canales J, Copaja M, Troncoso R, Vicencio JM, Carrillo C, et al. Beta(2)-adrenergic receptor regulates cardiac fibroblast autophagy and collagen degradation. Biochim Biophys Acta. 2011;1812(1):23-31.
- 35. Pan J, He L, Li X, Li M, Zhang X, Venesky J, et al. Activating Autophagy in Hippocampal Cells Alleviates the Morphine-Induced Memory Impairment. Mol Neurobiol. 2017;54(3):1710-24.
- 36. Sil S, Periyasamy P, Guo ML, Callen S, Buch S. Morphine-Mediated Brain Region-Specific Astrocytosis Involves the ER Stress-Autophagy Axis. Mol Neurobiol. 2018;55(8):6713-33.
- 37. Leuner B, Shors TJ. Stress, anxiety, and dendritic spines: what are the connections? Neuroscience. 2013;251:108-19.
- 38. Xiao X, Shang X, Zhai B, Zhang H, Zhang T. Nicotine alleviates chronic stress-induced anxiety and depressive-like behavior and hippocampal neuropathology via regulating autophagy signaling. Neurochem Int. 2018;114:58-70.
- 39. Woo M, Choi HI, Park SH, Ahn J, Jang YJ, Ha TY, et al. The unc-51 like autophagy activating kinase 1-autophagy related 13 complex has distinct functions in tunicamycin-treated cells. Biochem Biophys Res Commun. 2020;524(3):744-9.

- 40. Zhang H, Shang Y, Xiao X, Yu M, Zhang T. Prenatal stress-induced impairments of cognitive flexibility and bidirectional synaptic plasticity are possibly associated with autophagy in adolescent male-offspring. Exp Neurol. 2017;298(Pt A):68-78.
- 41. Feng J, Yan Z, Ferreira A, Tomizawa K, Liauw JA, Zhuo M, et al. Spinophilin regulates the formation and function of dendritic spines. Proc Natl Acad Sci U S A. 2000;97(16):9287-92.
- 42. Sarrouilhe D, di Tommaso A, Metaye T, Ladeveze V. Spinophilin: from partners to functions. Biochimie. 2006;88(9):1099-113.
- 43. Fourla DD, Papakonstantinou MP, Vrana SM, Georgoussi Z. Selective interactions of spinophilin with the C-terminal domains of the delta- and mu-opioid receptors and G proteins differentially modulate opioid receptor signaling. Cell Signal. 2012;24(12):2315-28.
- 44. Kallergi E, Nikoletopoulou V. Macroautophagy and normal aging of the nervous system: Lessons from animal models. Cell stress. 2021;5(10):146-66.
- 45. Lalanne L, Ayranci G, Kieffer BL, Lutz PE. The kappa opioid receptor: from addiction to depression, and back. Front Psychiatry. 2014;5:170.
- 46. Tejeda HA, Shippenberg TS, Henriksson R. The dynorphin/kappa-opioid receptor system and its role in psychiatric disorders. Cell Mol Life Sci. 2012;69(6):857-96.
- 47. Jacobson ML, Wulf HA, Browne CA, Lucki I. The kappa opioid receptor antagonist aticaprant reverses behavioral effects from unpredictable chronic mild stress in male mice. Psychopharmacology (Berl). 2020;237(12):3715-28.
- 48. Tang G, Gudsnuk K, Kuo SH, Cotrina ML, Rosoklija G, Sosunov A, et al. Loss of mTOR-dependent macroautophagy causes autistic-like synaptic pruning deficits. Neuron. 2014;83(5):1131-43.
- 49. Domi E, Barbier E, Augier E, Augier G, Gehlert D, Barchiesi R, et al. Preclinical evaluation of the kappa-opioid receptor antagonist CERC-501 as a candidate therapeutic for alcohol use disorders. Neuropsychopharmacology. 2018;43(9):1805-12.
- 50. Morou E, Georgoussi Z. Expression of the third intracellular loop of the delta-opioid receptor inhibits signaling by opioid receptors and other G protein-coupled receptors. J Pharmacol Exp Ther. 2005;315(3):1368-79.
- 51. Carlin RK, Grab DJ, Cohen RS, Siekevitz P. Isolation and characterization of postsynaptic densities from various brain regions: enrichment of different types of postsynaptic densities. J Cell Biol. 1980;86(3):831-45.
- 52. Carey MF, Peterson CL, Smale ST. Chromatin immunoprecipitation (ChIP). Cold Spring Harb Protoc. 2009;2009(9):pdb prot5279.

Figure legends

Φιγυρε 1: Αςτιατιον οφ τηε χ-ΟΡ ινδυςες τηε αυτοπηαγις μαςηινερψ ιν νευροναλ ςελλς. χ-Neuro2A cells were (A) treated with various concentrations of U50,488H (10, 20, 50 μM) for 6 h, (B) pre-treated with 20 nM BafA1 for 16 h, prior to U50,488H (20 μM) exposure for 6 h. (C) χ-Neuro-2A cells were pre-treated with 50 μM naloxone for 45 min, prior to U50,488H (20, 50 μM) exposure for 6 h. All cell lysates (50 μg) were subjected to 17 % SDS-PAGE for western immunoblotting to detect the autophagosome formation, (top panels, immunoblots of LC3-II and β-actin; bottom panels, quantification of LC3-II (measured with an anti-LC3B antibody and normalized to β-actin levels). (D) Primary neuronal cultures were pre-treated or not with naloxone (50 μM) for 45 min and exposed to U50,488H (50 μM) for 6h. Confocal images of 10 DIV embryonic cortical neurons, immunostained with an anti-LC3B antibody (1:200) to label autophagosomes, MAP2 (1:500) to label dendrites, and the nuclear dye, Hoechst (1:1000). (E)Embryonic primary neuronal cultures were administered for 6 h with the indicated concentrations of U50,488H (lanes 2-4). Lane 5, represents lysates from neuronal cultures treated with 50 μM naloxone prior

to U50,488H administration. Top panel represents immunoblots of LC3-II and β -actin. Quantification of LC3-II was normalized to β -actin levels (bottom panel). All experiments were performed independently at least 3 times. Error bars represent mean values \pm SEM. Statistical analysis was performed using Statistical analysis was performed using one or two-way ANOVA. *p < 0.05 and **p<0.01 as compared in the absence of agonist, #p<0.05 as compared with samples in the presence of U50,488H.

Φιγυρε 2. Δψνορπηιν ινδυςες κ-OP-μεδιατεδ αυτοπηαγψ ιν νευροναλ ςελλς. (A, B) κ-Neuro-2A cells were treated with various concentrations (0.1, 1 and 20 μM) of dynorphin₁₋₁₃ for 3 and 6 h. The levels of LC3-II (A) and Beclin1 (B)after dynorphin₁₋₁₃ treatment for 6 h were detected by western blotting. Data represent mean±SEM of three independent experiments; Statistical analysis was performed using one-way ANOVA. *p<0.05 as compared to untreated samples. (C) κ-Neuro-2A cells were pre-treated for 1 h, with or without the κ-OR antagonist nor- (5 μM) following administration with 1 μM dynorphin for 6 h. The LC3-II levels were detected by western blotting. β-actin served as loading control. Error bars represent mean± of three independent experiments, *p < 0.05 as compared with untreated samples. #p<0.05 as compared with samples in the presence of nor-. Statistical analysis was performed using two-way ANOVA. (D) Representative confocal images of embryonic DIV 10 neurons were treated or not with 1 μM dynorphin for 6 h and immmunostained with antibodies against LC3B (1:200) and Tuj1 (1:1000) to label autophagosomes and mature dendrites respectively and the nuclear dye TO-PRO3 (1:500). Statistical analysis was performed using one-way ANOVA. **p < 0.01 as compared with untreated cells.

Figure 3: U50,488H treatment of neuronal cultures upregulates autophagosome biogenesis. (A) Primary neuronal cultures were treated with 20 μM U50,488H for 1, 6, and 24 h and the levels of pre-autophagic markers FIP200 (1:1000) and Ulk1(1:1000) were identified by western blotting using the corresponding antibodies. (B) Western blot analysis against Beclin1 antibody and normalized with β-actin of Neuro-2A cell lysates after 20 μM U50,488H treatment at the indicated time intervals. (C) \varkappa -Neuro2A cells were treated with 20 and 50 μM U50,488H for 6 h and the levels of ATG5 (1:1000), Beclin1 (1:1000) and p62 (1:1000) were detected by western blotting against the corresponding antibodies. (D) \varkappa -Neuro2A cells were treated with 20 μM U50,488H for 6 h and the mRNA levels of Becn1 and Atg5 were examined by real-time PCR. Error bars represent average \pm SEM.Statistical analysis was performed using one way ANOVA. All experiments were performed at least three times. *p < 0.05 as compared with untreated samples.

Φίγυρε 4: χ-OP αςτιατίον ινδύζες αυτοπήαγ ψ ιν α $\Gamma_{\iota/o}$ προτείν, EPK 1,2 χίνασε ανδ π-"PEB δεπενδεντ μαννερ. κ-Neuro2A cells were pre-treated with PTX (100 ng/ml) for 16 h, followed exposure to U50,488H (20, 50 µM) for 6 h. LC3-II levels (A) were assessed in protein lysates by western immunoblotting. (B)Beclin1 levels were detected after PTX pretreatment following administration with 20 μΜ U50,488H for 6 h. (C) x-Neuro2A cells were pre-treated with PTX for 16 h, prior to U50,488H (20 μM) for 15 min and 6 h exposure and the levels of p-ERK1,2 were quantified. Tubulin was used as loading control. (D) x-Neuro2A cells were pre-treated with the ERK1,2 inhibitor PD98059 (20 µM) for 2 h, followed by U50,488H (20 µM) administration for 6 h. Total ERK1,2 was used for quantification. (E) The levels of p-JNK were estimated in x-Neuro2A cells in the presence or not of 20 µM of the JNK inhibitor SP600125 for 30 min prior to 6 h U50,488H (20 µM) administration. All experiments were performed three times. Error bars represent mean values±SEM. Statistical analyses were performed using two-way ANOVA. *p < 0.05 as compared with untreated cells, #p<0.05 as compared with samples with U50,488H alone. (F) x-Neuro-2A cells were pre-treated with or without PD98059 (20 µM) for 2 h, followed by U50,488H (20 µM) exposure for 6 h. The phosphorylated levels of CREB were analyzed by western blotting using an anti-p-CREB (Ser133) (1:500) serum and quantified using a CREB antibody (1:1000). Statistical analysis was performed using two-way ANOVA. *p < 0.05 as compared with untreated samples and #p<0.05 as compared with samples in the presence of U50,488H. (G) Chromatin immunoprecipitation was performed in x-Neuro-2A cells as described in Materials and methods using an anti-CREB (10 µg) (lanes 3, 4) or normal rabbit serum (NRS) (lanes 1, 2) and immunoprecipitated Becn1 was quantified by PCR on an agarose gel.

Φίγυρε 5: κ -OP αςτιατίον ινδύςες αυτοπήαγψ ιν μουσε ηιπποςαμπύς ανδ αλτέρς σψυαπτοσομάλ πρότειν λέελς. Male mice were injected i.p. with saline (vehicle) or 5 mg/kg U50,488H

for six consecutive days and the hippocampus (A), cortex (B) and striatum(C) were isolated and lysed as described in Materials and methods. Autophagosome accumulation was measured by western blotting using LC3B and Beclin1 antibodies. Brain lysates from hippocampus(D), cortex (E), and striatum (F) of saline-and U50,488H-injected mice were isolated and the protein levels of spinophilin (1:000) and PSD-95 (1:1000), were measured by immunoblotting using the corresponding antibodies. β -tubulin (1:000) was used as loading control. (G) Hippocampal synaptosomes of saline- or U50,488H-injected mice were isolated and the levels of spinophilin, PSD-95, and SNAP-25 were detected using the corresponding antibodies and quantified by Image J software using β -actin. All data are presented as average \pm SEM from three independent experiments (n=4/group, *p < 0.05 as compared with saline group using one-way ANOVA with post-hoc test).

Figure 6. χ-ΟΡ-μεδιατεδ αυτοπηαγψ λεαδς το δεγραδατιον οφ σψναπτοσομαλ προτεινς. (A) Hippocampal lysates (800 μg) were immunoprecipitated with 2 μg of an LC3B antibody and immunoblotted with spinophilin, PSD95 and SNAP25. NRS immunoprecipitated samples were used as negative control. (B) χ-Neuro-2A cells were pre-treated with 20 nM BafA1 for 24 h, following exposure with 20 μM U50,488H for 16 h. Cell lysates were subjected to 10% SDS-PAGE and the protein levels of spinophilin, PSD95 and SNAP25 were detected using the corresponding antibodies. Quantification of the synaptic proteins was normalized using β-tubulin. Error bars represent mean values ± SEM of three independent experiments. Statistical analysis was performed using one-way ANOVA, *p < 0.05 as compared with the values in the absence of agonist.(C) Primary hippocampal neuronal cultures were treated for 24 h with 20 μM U50,488H and labeled with a βIII-tubulin (Tuj1) antibody (1:1000). Nuclei were stained with TO-PRO-3 (blue) (1:500). Graph represents mean ± S.E.M of the number of branches calculated from 100 Tuj1-positive neurons of control and U50,488H-treated neuronal cultures; scale bar: 40 μm. Statistical analysis was performed using one-way ANOVA, ***p<0.001 as compared with the untreated samples.

Figure 7: Nor-BNI blocks FST-induced autophagy promoting synaptic alterations in mouse hippocampus. (A) Experimental timeline of the nor-BNI administration protocol and the 2-day repeated FST in C57BL/6J mice. Four groups of animals [saline and nor-BNI (non-stressed groups), and saline and nor-BNI exposed to FST (stressed groups)], (n=6/group) were injected i.p. with saline or the specific χ-OR antagonist nor-BNI (10 mg/kg) on day 1. One hour after injection, mice were subjected to 15 min FST. On the second day, mice were subjected to 4x 6 min FST trials and immediately sacrificed and hippocampi and cortices were isolated. (B) For behavioral analysis the immobility time of mice was quantified using a video tracking software as described in Materials and Methods. Statistical analysis was performed by one-way ANOVA variance, *p<0.05 relative to FST saline group. For autophagy induction, LC3-II and Beclin 1 levels were measured in hippocampus (C) and cortex(D) with Western immunoblotting. (E) The levels of spinophilin, PSD-95 and SNAP-25 in the hippocampus were detected from the four groups to evaluate differences between the stressed and non-stressed animals injected with saline or nor-BNI. β-tubulin was used as the loading control. (F) Spinophilin, PSD-95 and SNAP25 levels were detected from isolated cortical lysates (50 µg) from the four mice groups. All data are presented as average \pm SEM (n=6/group *p < 0.05 as compared with the saline non-stressed group and $^{\#}p < 0.05$ compared with the saline stressed ones using two-way ANOVA with post-hoc test).

Figure 8: Σςηεματις ρεπρεσεντατιον οφ α πυτατιε σιγναλινή πατήμαψ ια ωηιςή χ-OP αςτιατίον τριγήερς αυτοπήαγψ ρεσυλτινή ιν σψναπτις αλτερατίονς. Agonist activation of χ-OR in neuronal cells leads to ERK1, 2 phosphorylation mediated by Gi/o proteins. Activated ERK1,2 subsequently phosphorylates CREB which in turn translocates to the nucleus to activate *Becn1* gene expression. Upregulation of Beclin1 and Atg5 promotes the initiation of autophagy resulting in alterations of hippocampal synaptic proteins enriched in dendritic spines.

Acknowledgments

We are grateful to Drs Kostas Iatrou and Ioannis Sotiropoulos (Institute of Biosciences and Applications) for critical reading the manuscript and valuable comments. We also thank Gregory Kafetzopoulos and Antonis Myridakis members of the Georgoussi's lab for technical assistance.

Data availability

The experimental data generated and/or analyzed during the current study are available from the corresponding author upon reasonable request.

Funding

This work was supported by the General Secretariat of Research and Technology (GSRT) grant «Excellence » NO-ALGOS-3722 to Z.G. We also acknowledge the support by the "OPENSCREEN-GR" "An Open-Access Research Infrastructure of Chemical Biology and Target-Based Screening Technologies for Human and Animal Health, Agriculture and the Environment" (MIS 5002691), which is implemented under the Action "Reinforcement of the Research and Innovation Infrastructure", funded by the Operational Programme "Competitiveness, Entrepreneurship and Innovation" (NSRF 2014-2020) and co-financed by Greece and the European Union (European Regional Development Fund). ZG, CK, AlS are members of the European COST Action CA18133, "ERNEST" a European Research Network on Signal Transduction and were supported to present the data.

Author contributions

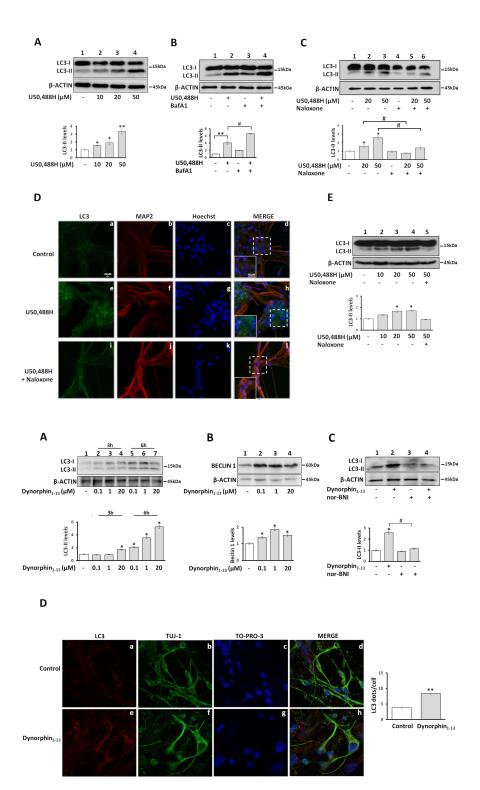
CK, designed and performed the experiments, analyzed the data and contributed to manuscript writing; AS, AlS, DPD, performed experiments; AVP, CK performed the behavioral studies; VN contributed to the data research, ZG supervised the study, analyzed data and wrote the manuscript. All authors have read and approved the final manuscript.

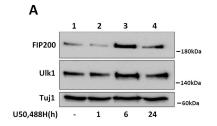
Conflict of interest

The authors declare no competing interests.

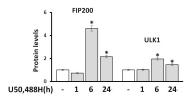
Ethics statement

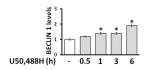
All animal experiments complied with the Greek Government animal experimental regulations and ARRIVE guidelines. The protocols were approved by the Ethics Committee of the National Centre for Scientific Research "Demokritos".











C

